Solar Powered Flight on Venus

Anthony Colozza
Analex Corporation, Brook Park, Ohio

The NASA STI Program Office . . . in Profile

Since its founding, NASA has been dedicated to the advancement of aeronautics and space science. The NASA Scientific and Technical Information (STI) Program Office plays a key part in helping NASA maintain this important role.

The NASA STI Program Office is operated by Langley Research Center, the Lead Center for NASA's scientific and technical information. The NASA STI Program Office provides access to the NASA STI Database, the largest collection of aeronautical and space science STI in the world. The Program Office is also NASA's institutional mechanism for disseminating the results of its research and development activities. These results are published by NASA in the NASA STI Report Series, which includes the following report types:

- TECHNICAL PUBLICATION. Reports of completed research or a major significant phase of research that present the results of NASA programs and include extensive data or theoretical analysis. Includes compilations of significant scientific and technical data and information deemed to be of continuing reference value. NASA's counterpart of peer-reviewed formal professional papers but has less stringent limitations on manuscript length and extent of graphic presentations.

- TECHNICAL MEMORANDUM. Scientific and technical findings that are preliminary or of specialized interest, e.g., quick release reports, working papers, and bibliographies that contain minimal annotation. Does not contain extensive analysis.

- CONTRACTOR REPORT. Scientific and technical findings by NASA-sponsored contractors and grantees.

- CONFERENCE PUBLICATION. Collected papers from scientific and technical conferences, symposia, seminars, or other meetings sponsored or cosponsored by NASA.

- SPECIAL PUBLICATION. Scientific, technical, or historical information from NASA programs, projects, and missions, often concerned with subjects having substantial public interest.

- TECHNICAL TRANSLATION. English-language translations of foreign scientific and technical material pertinent to NASA's mission.

Specialized services that complement the STI Program Office's diverse offerings include creating custom thesauri, building customized databases, organizing and publishing research results . . . even providing videos.

For more information about the NASA STI Program Office, see the following:

- Access the NASA STI Program Home Page at *http://www.sti.nasa.gov*

- E-mail your question via the Internet to help@sti.nasa.gov

- Fax your question to the NASA Access Help Desk at 301–621–0134

- Telephone the NASA Access Help Desk at 301–621–0390

- Write to:
  NASA Access Help Desk
  NASA Center for AeroSpace Information
  7121 Standard Drive
  Hanover, MD 21076

NASA/CR—2004-213052

Solar Powered Flight on Venus

Anthony Colozza
Analex Corporation, Brook Park, Ohio

National Aeronautics and
Space Administration

Glenn Research Center

April 2004

Solar Powered Flight on Venus

Anthony Colozza
Analex Corporation
Brook Park, Ohio 44212

Abstract

Solar powered flight within the Venus environment from the surface to the upper atmosphere was evaluated. The objective was to see if a station-keeping mission was possible within this environment based on a solar power generating system. Due to the slow rotation rate of Venus it would be possible to remain within the day light side of the planet for extended periods of time. However the high wind speeds and thick cloud cover make a station-keeping solar powered mission challenging. The environment of Venus was modeled as a function of altitude from the surface. This modeling included density, temperature, solar attenuation and wind speed. Using this environmental model flight with both airships and aircraft was considered to evaluate whether a station-keeping mission is feasible. The solar power system and flight characteristics of both types of vehicles was modeled and power balance was set up to determine if the power available from the solar array was sufficient to provide enough thrust to maintain station over a fixed ground location.

Introduction

Flight within the Venus atmosphere provides a unique and valuable means for scientific investigation of the planet. Due to the harsh environmental conditions near the surface, few science probes or surface landers have been sent to Venus. Orbiting satellites, such as Magellan, and spacecraft flybys have been the main means of exploring the planet. However, because of the planet's thick atmosphere and abundant solar radiation due to its proximity to the sun, solar powered flight within the atmosphere can be considered.

Flight vehicles can provide a unique perspective for the exploration of Venus. Because they would be powered by the sun, their mission times would be on the order of Earth months. This is considerably longer than what is achievable using probes that would only have a lifetime of hours at best. In addition to long mission times, controlled flight within the atmosphere provides a means of investigating specific areas of the atmosphere. A number of potential science missions can be carried out by solar powered flight vehicles. Some examples of these would be:

- The collection of atmospheric properties over a region of the atmosphere
- Direct sampling of the atmosphere
    - Provide information on atmospheric makeup
    - Look for trace biogenic gasses as indicators of life
- Magnetic field mapping over a region of the planet
- Visual imagery
- Communications and command relay for surface vehicles and landers.

To perform the types of science exploration listed above, two types of solar powered vehicles can be considered. These are airships and aircraft. Airships generate lift through buoyancy force whereas aircraft generate lift through the aerodynamics of fluid flow over the wings. If feasible, each type of vehicle would provide a means of controlled flight within the Venus atmosphere. To examine their feasibility, a detailed understanding of the planet's atmospheric conditions is necessary. Items such as solar intensity, wind speed and density as a function of altitude are necessary to assess whether controlled flight is possible for each type of vehicle. Since the power for flight and operations comes solely from the sun, the

feasibility will be based on a balance between the available power from the solar array and the power required to maintain flight at speeds greater then the wind speed at a specific altitude.

Using this approach, both solar powered airships and aircraft were examined to determine if and where they were capable of flight. A minimum mission duration of 50 days was set as the operational time for each vehicle and altitude being examined. The goal was to provide a flight envelope where controlled flight can be sustained for each type of vehicle by examining operation from the surface to the upper atmosphere (approximately 80 km).

Environmental Conditions

Venus, shown in figure 1, is the third planet from the sun and has a number of unique characteristics that makes its environment both interesting and challenging for flight. The basic physical and orbital properties of Venus are given in table 1. Venus is very similar in size to Earth. However this is where the similarities end. The environmental conditions on Venus are very unique and unlike those on any other known planet or moon. Venus has a very thick atmosphere with cloud cover over the entire planet. However, strange as this may seem, Venus may be an ideal place to fly a solar powered air vehicle. That is because the cloud cover only extends from approximately 45 km above the surface to approximately 64 km above the surface. At the top of the cloud layer, the atmospheric pressure is around 0.1 bar. Within this altitude range, the atmospheric temperatures are between 80 °C to –35 °C respectively. The temperature profile on Venus is shown in figures 2 and 3 [1]. Operation within this temperature range of the upper atmosphere will not be an issue. In fact, operation at the colder end of the range will increase the solar array performance. The top of the cloud layer corresponds to a pressure altitude of 16 km (52,500 ft) on Earth. Although high, this altitude is well within the range of modern aircraft and flight aerodynamics within this regime are well understood [2]. The properties of the Venus atmosphere from the surface to 100 km are listed in Appendix A.
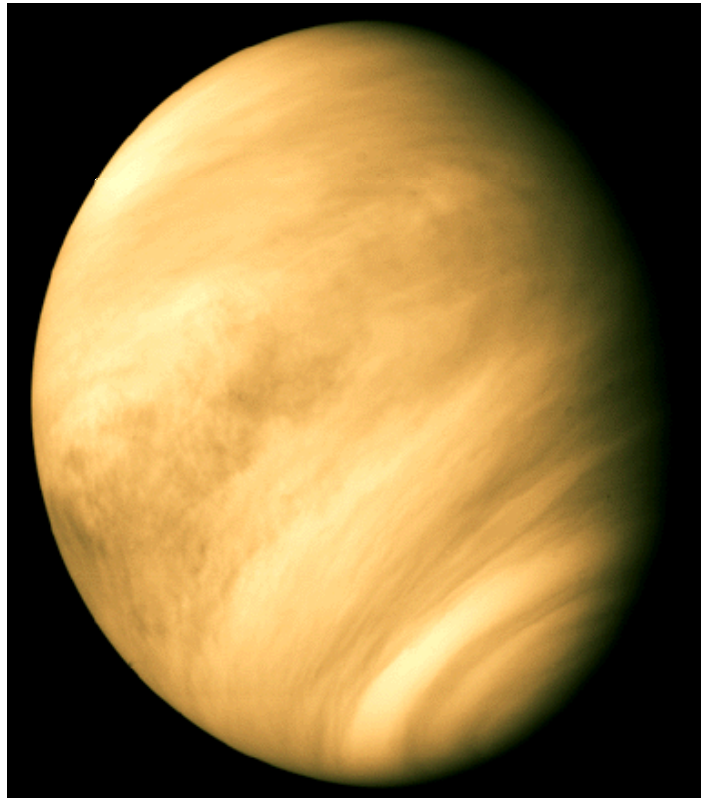

Figure 1.—Venus from space [1].

Table 1.—Physical and orbital properties of Venus [3].

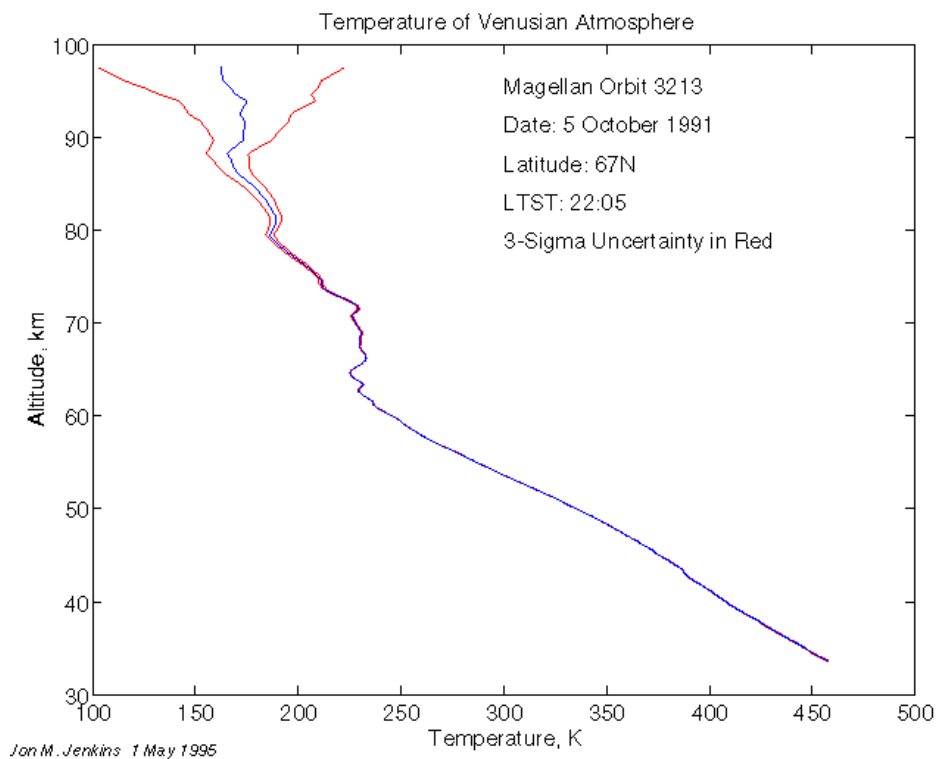| Property	Value
Maximum Inclination of Equator to Orbit (δ_{max})	**3.39°**
Orbital Eccentricity (ε)	**0.0067**
Mean Radius of Orbit (r_m)	**108E6**
Day Period	**243 (Earth Days)**
Solar Radiation Intensity	**Mean: 2613.9 W/m^2** **Parihelion: 2649 W/m^2** **Apehelion: 2579 W/m^2**
Albedo	**0.65**
Gravitational Constant (g)	**8.87 m/s^2**
Sidereal Year	**224 (Earth Days)**
Surface Temperature	**737 K**
Diameter	**12,104 km**

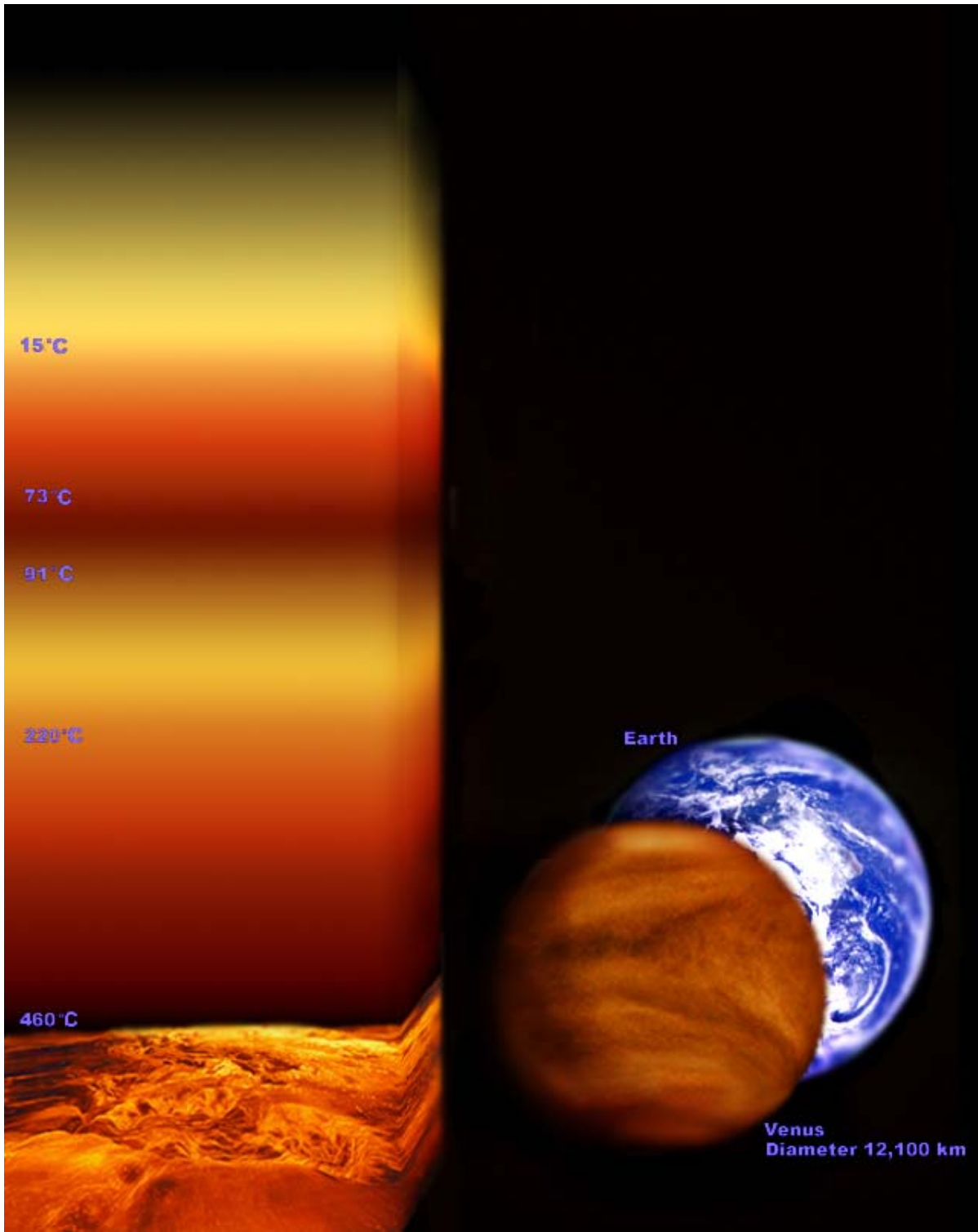Figure 2.—Temperature profile of Venus's atmosphere.

Figure 3.—Temperature profile within Venus's atmosphere [1].

Because of the thick atmosphere, the pressure and density throughout most of the atmosphere is much greater than that on Earth. The atmospheric pressure and density we experience near the surface of Earth occurs at an altitude of just over 50 km on Venus. For a flight vehicle, this means that flying at 50 km on Venus is similar aerodynamically to flying near the surface on Earth. The atmospheric density (ρ) within the Venus atmosphere can be represented by equation 1 as a function of altitude (h) in kilometers. This equation is plotted in figure 4.

$$\rho = 64.85 - 3.3257h + 0.067373h^2 - 0.00066981h^3 + 3.224E - 6h^4 - 5.6694E$$
$$-9h^5 - 1.8971E - 12h^6$$

(1)

Above the cloud layer there is an abundant amount of solar energy. The solar flux at the orbit of Venus is 2600 W/m^2, which is much greater than the 1360 W/m^2 available at Earth orbit. This nearly 100 percent increase in solar flux can significantly increase the performance of solar powered vehicles. Even within the cloud layer there may be sufficient solar energy to operate aircraft. At the bottom of the cloud layer (45 km altitude), the solar intensity is between 520 W/m^2 and 1300 W/m^2 depending on the wavelength of the radiation being collected. This is comparable to the solar intensity at Mars or Earth respectively. Therefore, even within the cloud layer, the ability to fly under solar power on Venus will be no worse than it is to fly on Earth or Mars.

The solar intensity as a function of altitude (h) in kilometers can be represented by the following equations. These equations represent a curve fit of attenuation [2] (I/I_o which is the ratio of the intensity at the selected altitude, I, to the solar intensity above the atmosphere, I_o) for the mid-spectrum wavelength of 0.72 μm.
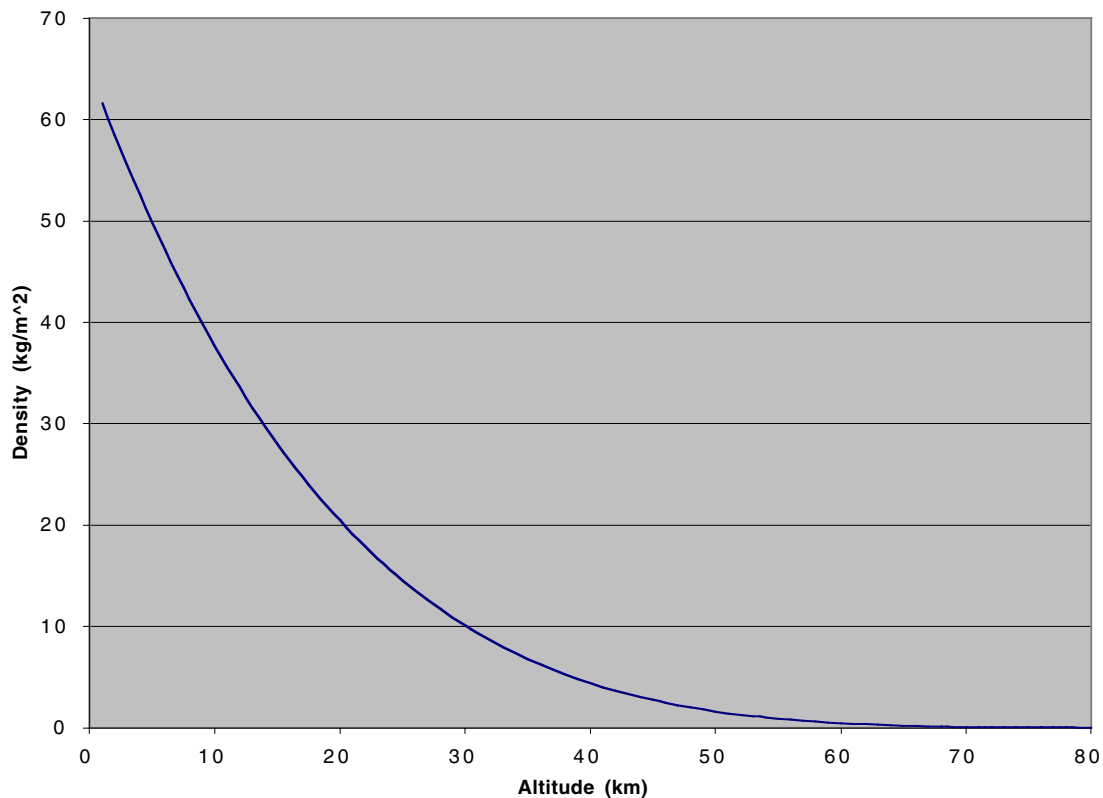

Figure 4.—Atmospheric density as a function of altitude.

From 0 to 50 km altitude:

$$I/I_o = 0.10306 + 0.017383h - 7.99E-4h^2 + 2.752E-5h^3 - 5.2011E-7h^4 + 3.874E-9h^5 \quad (2)$$

From 50 km to 65 km altitude:

$$I/I_o = -1.3639 + 0.036023h \quad (3)$$

Above 65 km there is effectively no attenuation and therefore τ has a value of 1. A graph of the solar attenuation as a function of altitude is shown in figure 5.

Another unique aspect of Venus is that the day length is longer then the year. Due to this slow rotational rate, the speed to remain at the same solar time is very low, approximately 13.4 km/hr. Therefore, it is conceivable that a solar powered aircraft or airship could remain within the sunlit portion of the planet indefinitely.

Overcoming the wind will be the key to maintaining the air vehicle's position within the sunlit portion of the planet. The winds within the atmosphere blow fairly consistently in the same direction as the planetary rotation (East to West) over all latitudes and altitudes up to 100 km. Above 100 km, the winds shift to blow from the day side of the planet to the night side. The wind speeds decrease as a function of altitude from ~100 m/s at the cloud tops (60 km) to ~0.5 m/s at the surface. These high wind speeds and the slow rotation of the planet produce a super rotation of the atmosphere (nearly 60 times faster then the surface). A curve fit of mean wind speed (V) in meters per second versus altitude (h) in kilometers was produced. This curve is given in equations 4 through 6 for the specified altitude ranges. A graph of the mean wind speed is also shown in figure 6.
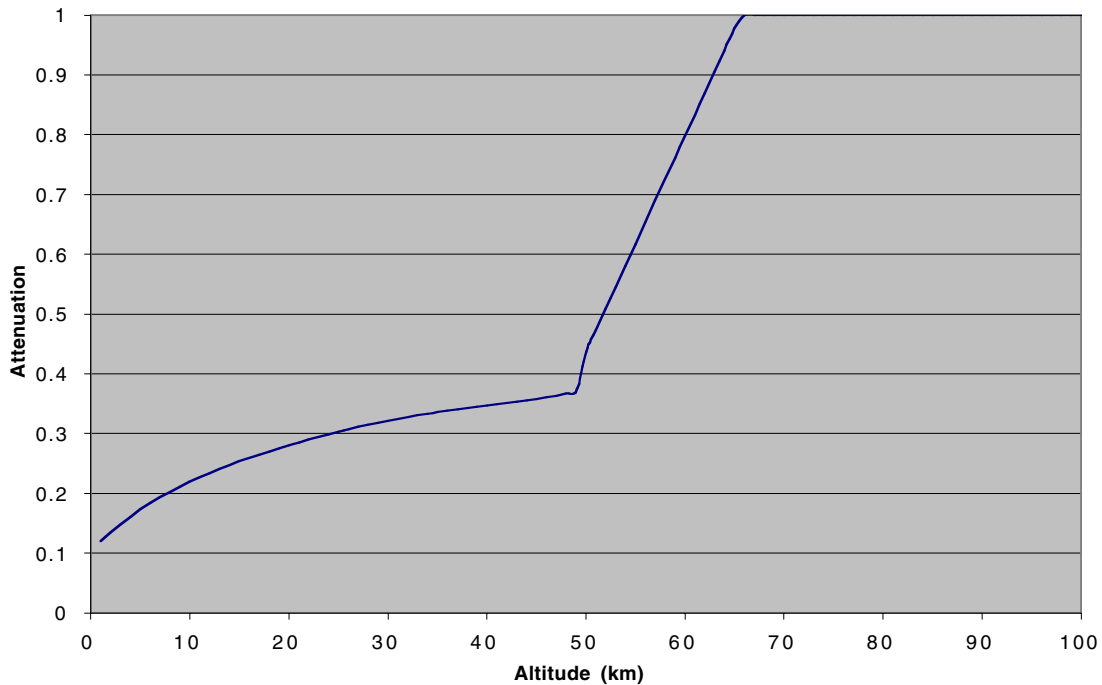

Figure 5.—Atmospheric solar attenuation as a function of altitude at 720 nm wavelength.
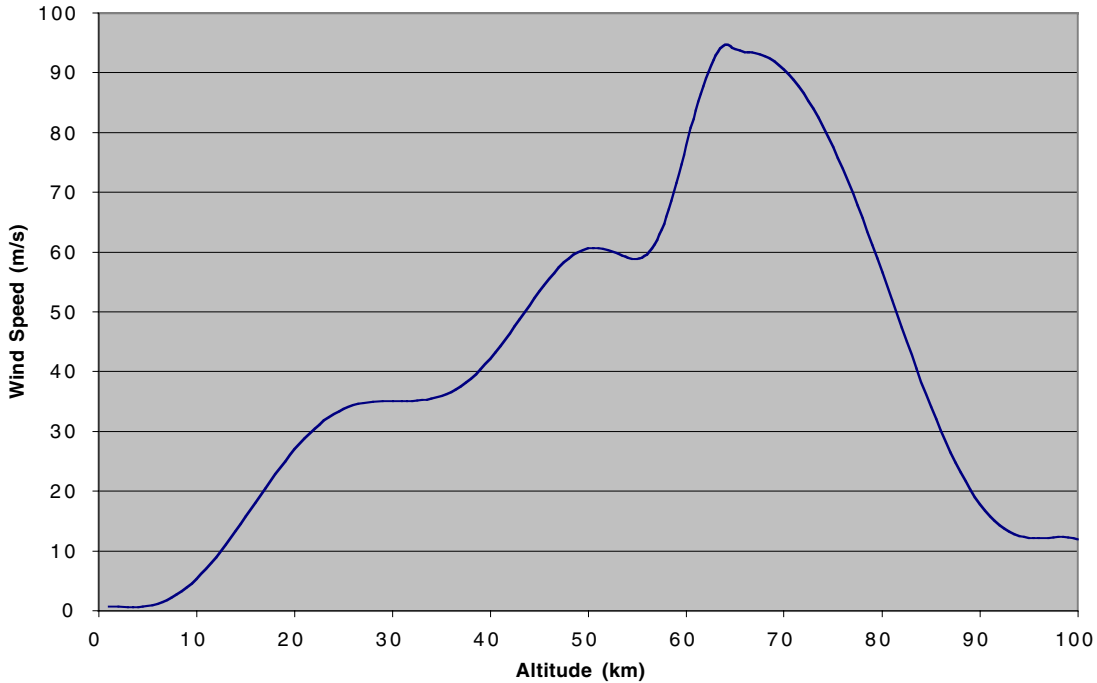
Figure 6.—Average wind speed versus altitude within the Venus atmosphere

From the surface to 58 km altitude:

$$V = 0.89941 - 0.11201h - 0.017082h^2 + 0.0040604h^3 + 0.0010345h^4$$
$$- 9.96E - 5h^5 + 3.28e - 6h^6 - 4.7E - 8h^7 + 2.495E - 10h^8 \tag{4}$$

From 58 km to 66 km altitude:

$$V = 21498 - 1087.9h + 18.31h^2 - 0.10214h^3 \tag{5}$$

From 66 km to 100 km altitude:

$$V = -3860.1 + 637.42h - 32.206h^2 + 0.76199h^3 - 0.009357h^4 + 5.783E - 5h^5 - 1.42E - 7h^6 \tag{6}$$

The gravitational acceleration on Venus (8.87 m/s²) is slightly less then that on Earth which aids somewhat in the lifting capability of the aircraft. The atmospheric composition on Venus can also pose problems for the aircraft. The atmosphere is composed mostly of CO_2 but also has trace amounts of corrosive compounds such as hydrochloric, hydrofluoric and sulfuric acids. [3] The atmospheric composition is given in table 2. Because of this composition, the speed of sound within the atmosphere is generally less then it is within Earth's atmosphere. The speed of sound (*a*) in meters per second as a function of altitude (*h*) above the surface in kilometers can be represented by equation 7 and is shown in figure 7 as a function of altitude.

$$a = 410.15 - 2.1102h + 0.008751h^2 - 0.00072086h^3 + 1.0136E - 5h^4 - 3.6825E - 8h^5 \tag{7}$$
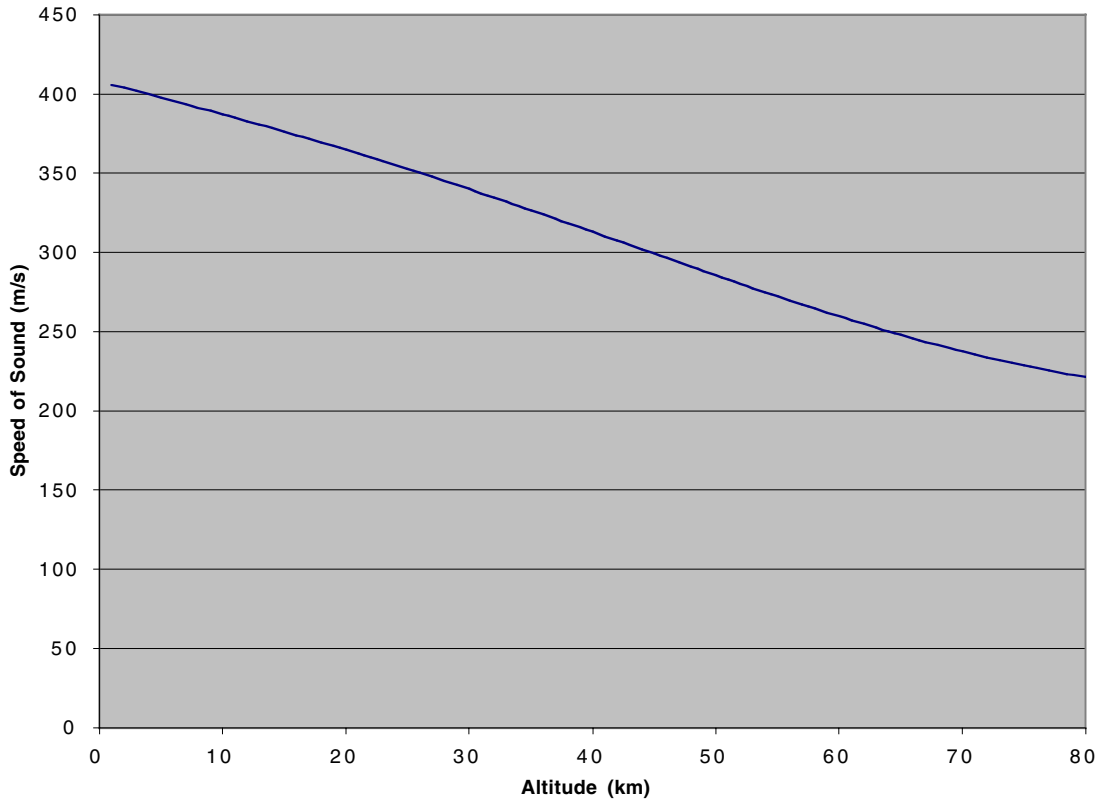
Figure 7.—Speed of sound as a function of altitude within the Venus atmosphere.

Table 2.—Venus Atmospheric Composition [4]

Gas	Percent Volume
Carbon Dioxide (CO_2)	96.5
Nitrogen (N_2)	3.5
Sulfur Dioxide (SO_2)	150 ppm
Carbon Monoxide (CO)	17 ppm
Water Vapor (H_2O)	20 ppm
Neon (Ne)	7 ppm
Argon (Ar)	70 ppm
Helium (He)	17 ppm

Solar Powered Airship

Due to the thick atmosphere on Venus, an airship is an obvious type of vehicle to consider for flight. To meet the mission goals and operate the airship for expended periods of time (50 or more days), solar arrays mounted on the upper surface of the envelope can be used to provide power. Although the high atmospheric density can provide significant buoyancy for the generation of lift, there are other characteristics of the environment that make operating a solar powered airship fairly difficult. These

include the thick cloud cover, high atmospheric temperature below the cloud layer, and the high winds within the upper atmosphere.

An evaluation of a solar powered airship was performed to determine if these environmental constraints could be overcome, and if so, what would be the necessary size and operating range of the airship. To begin the evaluation a basic airship configuration had to be assumed. The configuration chosen consists of a standard cylindrical shape with three tail fins and two propulsion pods. Solar arrays were located on the upper surface of the airship envelope and on the tail fins. This basic layout is shown in figure 8.

Using the atmospheric environmental conditions described previously, the operation of sizing an airship was performed from the surface to the upper atmosphere. The output of the solar array was calculated based on the incident solar radiation on the array [5]. The incident radiation is dependent on the shape of the array and the attenuation (figure 5) due to the atmosphere. Because of the thick atmosphere and cloud cover, it was assumed that all solar radiation below the clouds was diffuse. Therefore, there was no variation in array output based on array or airship position relative to the location of the sun. The array output or power available (P_a) is given in equation 8. It is based on the mean solar intensity at orbit (I_{om}, given in table 1) and the attenuation due to the atmosphere (I/I_o, given by equations 2 and 3).

$$P_a = I_{om}\left(\frac{I}{I_o}\right)A_{sc}\eta_{sc} \tag{8}$$

The total area of the solar array (A_{sc}) assumes that the array is placed on the upper half of the airship envelope (as shown in figure 8) and on the tail fin surfaces. The solar cell efficiency (η_{sc}) is based on the efficiencies of thin film solar cells and was assumed to be 5 percent. To determine the fin area, a number of existing airships were used to establish a ratio of fin area to airship volume. The ratio of fin area to airship volume used for this analysis was 0.0121 m^2/m^3. It is assumed that portions of the solar array would be located on the upper surface of the lower tow fins and on both sides of the vertical fin. Therefore, to get the surface area of the fins available for the placement of the solar array, the total fin area is multiplied by 4/3 for the three fin configuration shown in figure 8.
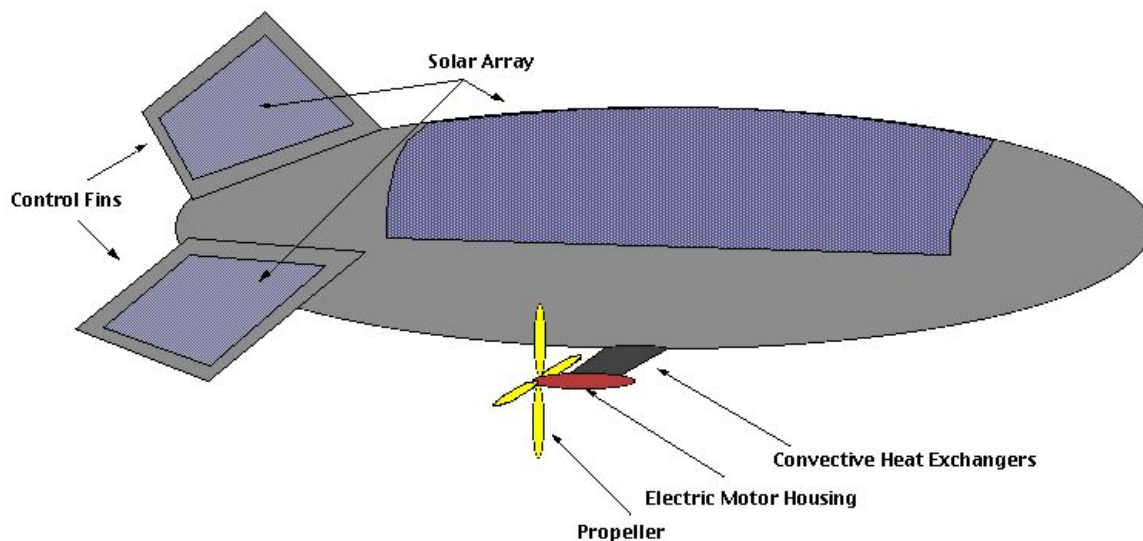

Figure 8.—Venus airship configuration.

The power required by the airship is given by the power needed to operate the onboard systems and payload and the power needed to overcome the drag on the airship and maintain station over a specified location. The airship drag (D), given in equation 9, is based on a volumetric drag coefficient (C_{dv}) and the airship volume (V_{as}). The volume can be determined from the length (l) and fineness ratio (f) of the airship. This relationship is given in equation 10. For this analysis, it was assumed that the airship was to maintain position. Therefore, the velocity (V) at which it is operating is the wind speed.

$$D = \frac{1}{2}\rho C_{dv} V^2 V_{as}^{2/3}$$ (9)

$$V_{as} = \pi L^3 \left(\frac{1}{4f^2} + \frac{4}{24f^3} \right)$$ (10)

The drag coefficient is based on the fineness ratio of the airship. The fineness ratio is the ratio of the length of the airship to its diameter (d) or width as given by equation 11. For this analysis a fineness ratio of 4 was assumed. The drag coefficient for this fineness ratio is 0.0266.

$$f = \frac{l}{d}$$ (11)

Due to the very low wind speeds near the surface of Venus, the majority of the power consumption of the airship comes from systems within the ship. These assumed power requirements are given in table 3.

Table 3.—Assumed system power levels.

System	Continuous Power Level
Communications	50 W
Control and Operations	50 W
Payload	50 W

The power for propulsion was estimated using the method given in reference 5. The total airship power level (propulsion power and all system power) is shown in figures 10 and 11.

Below the cloud layer, the availability of power is the driving factor for the airship design. Its size is based on the ability to collect enough power from the solar array to operate the propulsion system and other ship systems. The airship is therefore sized for this requirement. Using the mass-scaling relationships given in reference 5 and assuming helium as the lifting gas, mass estimates of the airship were made. Due to the high density environment of the Venus atmosphere, the lift produced by the envelope volume was more than sufficient to lift the airship and its associated systems. In fact much of the envelope would need to be filled with atmospheric gas with only a small volume utilized by the lighter lifting gas. Because of this, the mass scaling of the airship is not a critical factor in the analysis. The lifting capacity of an airship as a function of altitude is shown in figure 9 with helium as the lifting gas. This figure shows the total mass that can be lifted as a function of altitude and airship size.

Using the analysis outlined above, the power required for maintaining station above a specific location and the power available from the solar array was determined for airship sizes up to 20 m in length. Airships larger then 20 m in length were deemed not reasonable for autonomous deployment and operation within the Venus atmosphere. The power required and available was calculated from near the surface up to an altitude of 50 km. These results are shown in figure 10.
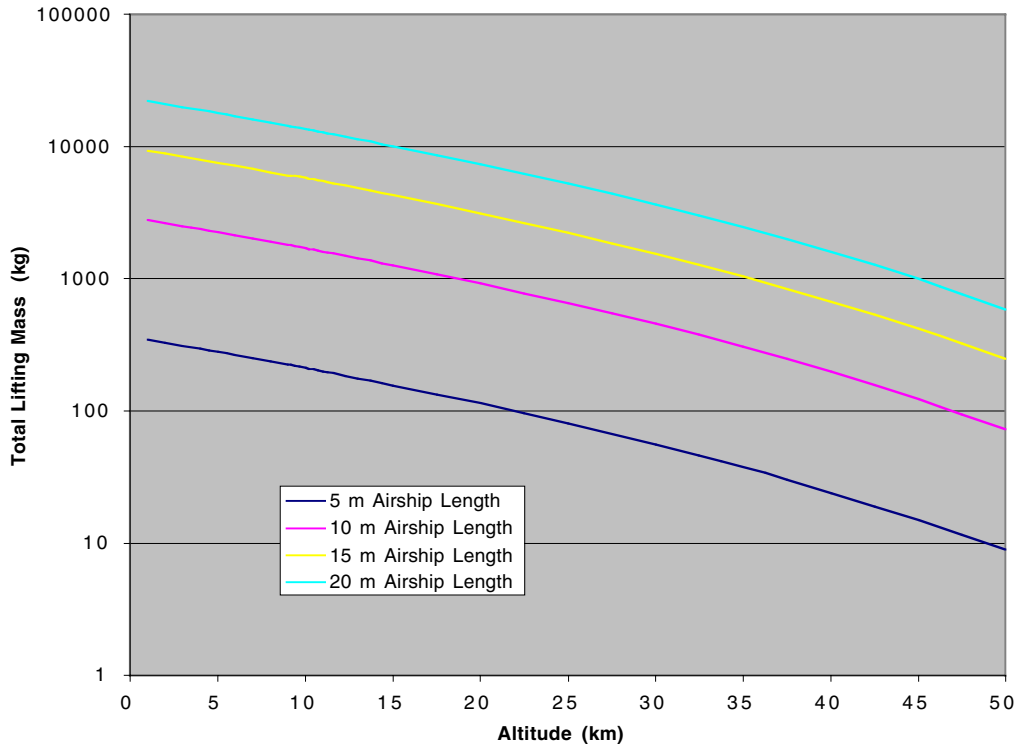
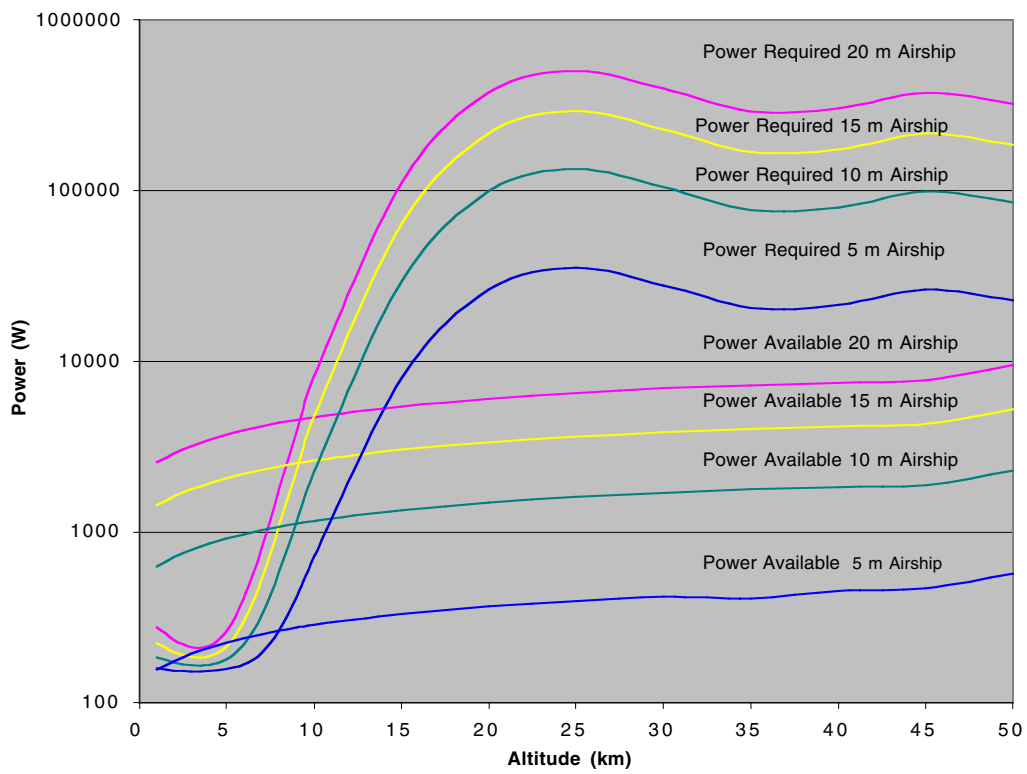Figure 9.—The lifting capacity of various size airships as a function of altitude.

Figure 10.—Power available and power required for various size airships.
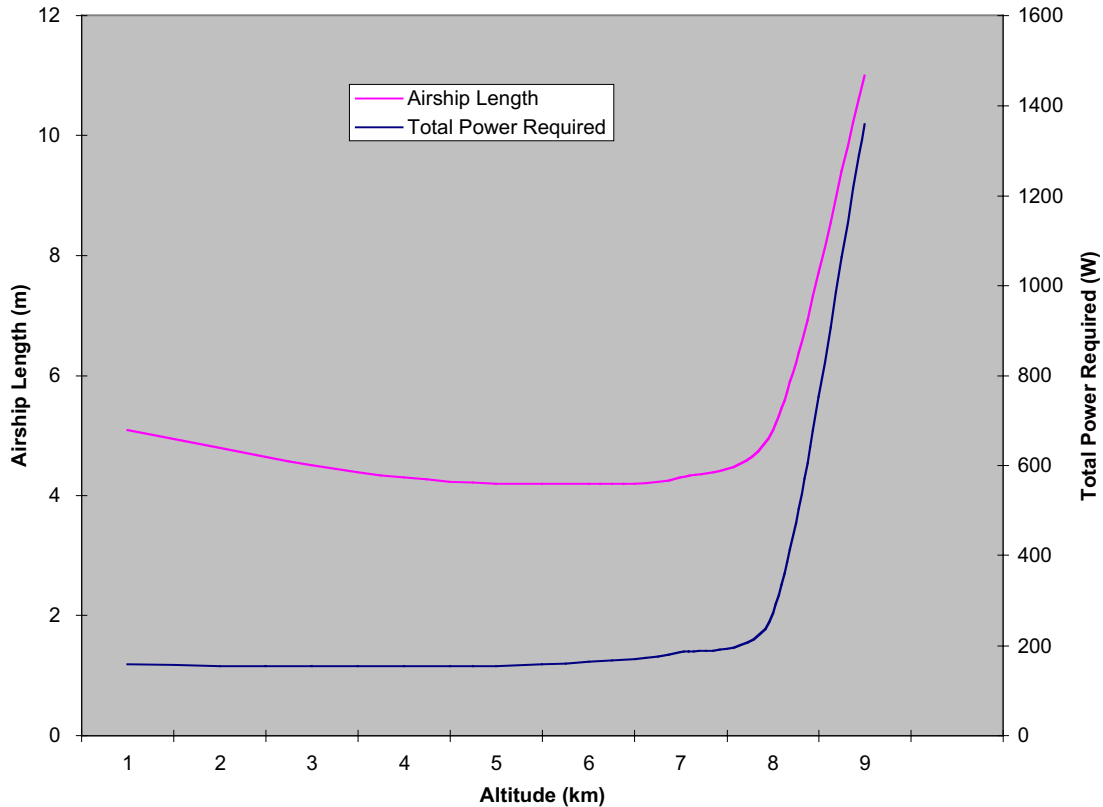
11

Figure 11.—Total power and airship size as a function of altitude on Venus.

From this figure it can be seen that there is a sharp rise in required power that occurs near 10 km in altitude. This rise is due to the increasing wind speeds that occur with increasing altitude as seen in figure 6. Because of this significant rise in the power required to maintain station, it is not feasible to operate a solar powered airship, of the sizes examined, above approximately 10 km in altitude. Below this altitude, the required airship size necessary to operate within the Venus environment was determined and is given in figure 11. This figure shows required airship size for altitudes up to 9 km.

Solar Powered Aircraft

As with the airship, the aircraft concept for flight on Venus will be solar powered. Because of the abundant solar energy available above the cloud layer and the desired mission duration of 50+ earth days, solar energy is the logical choice for powering an aircraft and will be the main power system considered in this analysis. The slow rotation rate of Venus, approximately 13.4 km/hr, presents a unique opportunity for a solar powered aircraft. This slow rate means that an aircraft will remain within the sunlit side throughout the mission, thereby eliminating the need for energy storage for nighttime operation. However there is one major obstacle to maintaining station over a given location, the upper level winds. Above the clouds, where there is abundant solar power, the wind speeds are very high, as shown in figure 6. These high average wind speeds mean that significant power will be required for the aircraft to maintain station over a specific location on the surface. So for a solar aircraft to be feasible for a station-keeping mission on Venus, it must be capable of producing enough thrust to overcome the wind speeds.

The flight altitude and aircraft size will depend on the power balance between the available power from the solar array and the drag of the aircraft due to flight at the velocity of the wind. The aircraft concept would be a standard wing tail arrangement with an electric motor driven propeller propulsion system. The main components of the propulsion system would consist of the solar array, a rechargeable

silver-zinc battery, power controller, electric motor, gearbox, and propeller. The main purpose of the battery within the system is to regulate the output power from the solar array, thereby providing continuous power at a near constant voltage to the main power bus of the aircraft. A diagram of the power and propulsion system for the aircraft is shown in figure 12 and a conceptual drawing of the aircraft is shown in figure 13.
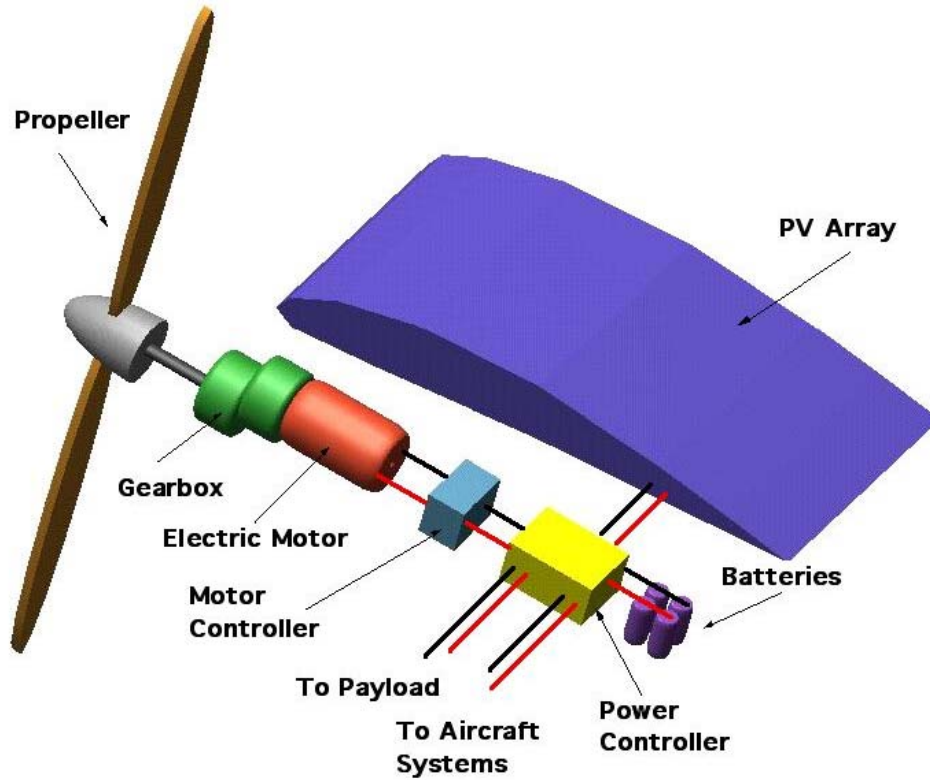
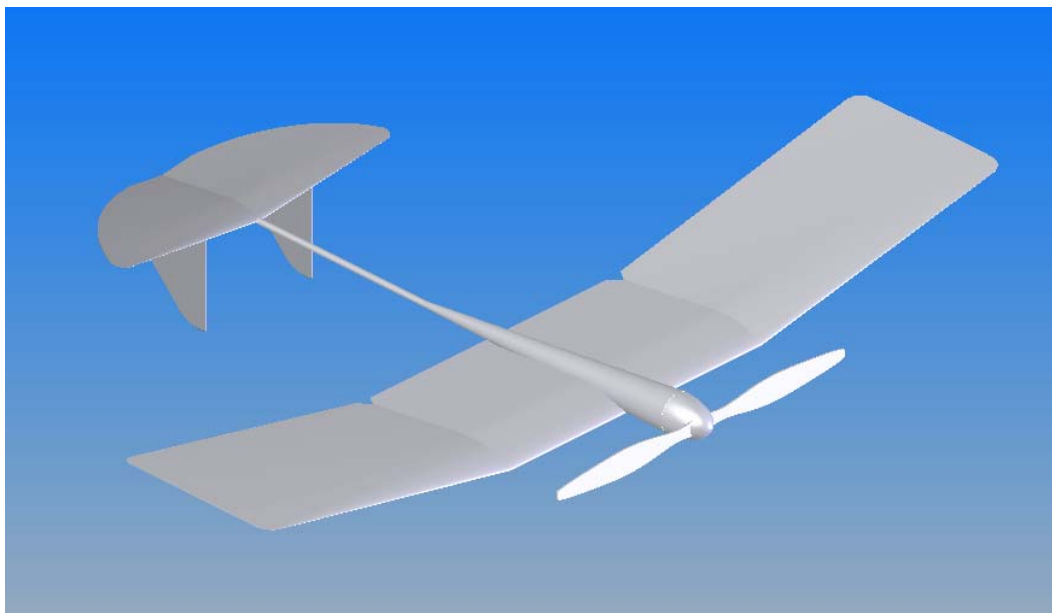

Figure 12.—Propulsion and power system layout.

Figure 13.—Venus aircraft conceptual drawing.

The first step in addressing the aircraft's size and flight altitude is determining the amount of power available for flight. The main power source for the aircraft is the sun. Photovoltaic arrays convert sunlight into electricity with is either stored in the silver-zinc battery or utilized directly for the aircraft operation. The amount of solar energy available is dependent on the location (or latitude) of the aircraft, the time of year, and any atmospheric attenuation (due to clouds, haze or dust). For the aircraft to operate, the power requirements will need to be less than what is available from the solar arrays. The power requirements include the power needed to generate thrust and the operational power for the aircraft that includes communications systems, flight control, and payload.

To determine the available power, some assumptions have to be made on the capabilities and geometry of the solar array and its power control system. These assumptions are listed in table 4. Also important in determining the total available power are the orbital and environmental characteristics of Venus. These are given in table 1.

Table 4.—Solar array characteristics and assumptions.

Characteristic	Value
Solar Cell Efficiency (η_{sc})	**18% at 20 °C**
Solar Cell Fill Factor (S_{ff})	**80%**
Power Conditioning Efficiency (η_{pcon})	**95%**
Horizontal Solar Array	**NA**
Solar Array on the Wing and Tail Surfaces	**NA**

The power available (P) per square meter of area is calculated as follows. The atmospheric attenuation (I/I_o) is given in figure 5 as a function of altitude. The solar cell efficiency (η_{sc}) will also vary with altitude and airspeed of the aircraft because of the change in operating temperature with different altitudes and flight speeds.

$$P = I_o \, (I/I_o) \, \eta_{sc} \, S_{ff} \, (S - C \cos(-\alpha)) \tag{12}$$

Where

$$S = \sin(\phi) \sin(\delta) \tag{13}$$

$$C = \cos(\phi) \cos(\delta) \tag{14}$$

The latitude (ϕ) and declination angle (δ) vary between zero and its maximum (δ_{max}) with the time of the year (t_y), that is defined as being between 0 and 1, beginning at an equinox. Since the day period is longer than the year, the time of the year is given as fractions of a year.

$$\delta = \delta_{max} \sin(2 \, \pi/t_y) \tag{15}$$

The angle (α) is given by the following expression, where the instantaneous time of the day (t_d) is also between 0 and 1, and is zero at the same equinox as the beginning of the year.

$$\alpha = 2 \, \pi \, t_d \tag{16}$$

$$I_o = I_{om} \, (r_m^2 / r^2) \tag{17}$$

The orbital distance from Venus to the sun (r) varies throughout the year. The planet's orbital radius is based on the mean radius (r_m) and is represented by equations 18 and 19, where the time of day is between 0 and 1, beginning at perihelion.

$$r = r_m \, (1 - e^2) / (1 + \varepsilon \cos(\theta)) \tag{18}$$

$$\theta = 2 \, \pi \, t_{dp} \tag{19}$$
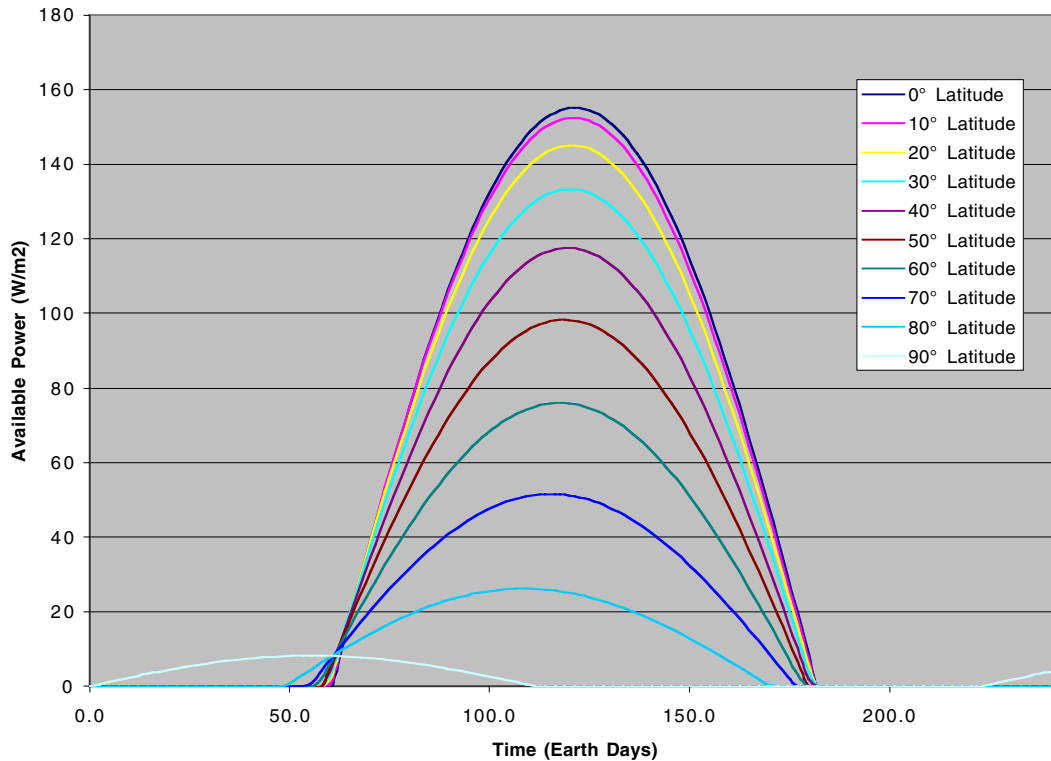
Figure 14.—Venus: available power throughout a day at various latitudes.

Based on the equations given above, the power available as a function of wing area can be determined. The power available to the aircraft at various latitudes on Venus is shown in figure 14 for an attenuation of 0.9 and a solar cell efficiency of 18 percent. The curves in this figure represent an example of the available power at different latitudes on Venus. The actual available power used in determining the flight envelope for the aircraft will be determined in a similar fashion for each flight altitude.

To determine if the available power at a given time and location is sufficient to operate the aircraft, an estimate of the power required to fly must be made. The power required for flight is given by equation 20 [7]. The first term in this equation represents the power needed to overcome the parasitic drag on the aircraft and the second term represents the power needed to overcome the induced drag due to the generation of lift.

$$P_r = \left(\frac{1}{2} \rho S_w c_{do} V^3 + \frac{2(Mg)^2}{\pi \rho e A_R S_w V} \right) \frac{1}{\eta_p}$$

(20)

The power required to fly is dependent on the characteristics of the aircraft, such as wing area (S_w), wing aspect ratio (A_r), total mass (M), drag coefficient (c_{do}), wing efficiency (e), propulsion system efficiency (η_p), and the environment in which it will fly. Because both the aircraft's available power (available solar flux) and its required power (wind velocity to maintain station) are dependent on the environment, sizing the aircraft for flight is an iterative process between variations in flight altitude and latitude and in the geometry of the aircraft. The sizing scheme for the aircraft is illustrated in figure 15.
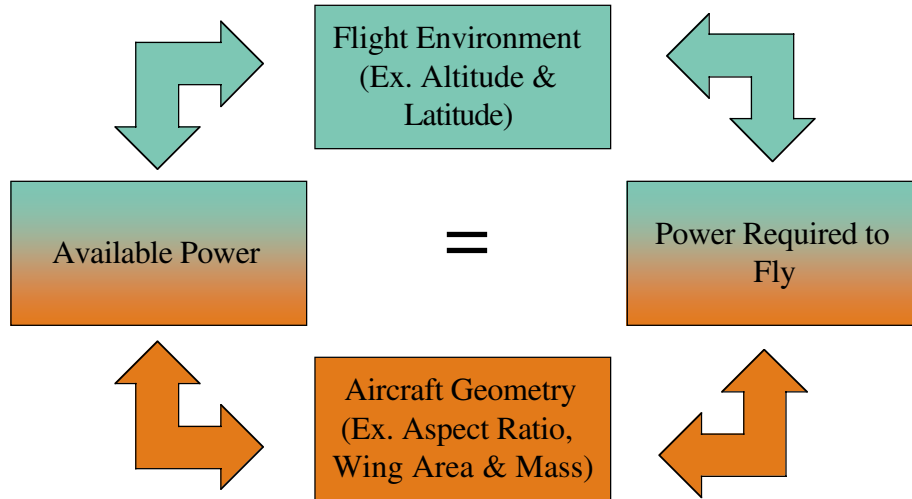
Figure 15.—Aircraft sizing logic diagram.

To determine the parasitic drag coefficient, the aircraft was broken down into five components: the wing, boom, vertical tail, horizontal tail and fuselage. The parasitic drag coefficient for each of these components was calculated and summed to get an estimate of the total parasitic drag coefficient for the aircraft. The total parasitic drag coefficient (c_{do}), which is the summation of the drag coefficients for each component (i), is based on the skin friction coefficient (c_f), the form factor (F) of the component, and its wetted surface area (S_{wet}). This relationship for total drag coefficient is given by equation 21 [8].

$$c_{do} = \frac{\sum_1^i c_{f_i} F_i S_{wet_i}}{S_w} \tag{21}$$

Assuming turbulent flow, which is a conservative estimate, the skin friction coefficient for each of the components can be represented by equation 22. This relation is based on the Reynolds number (Re), given in equation 23, of each of the component sections. The characteristic length for each of the components is in the flow-wise direction. For the wing, vertical, and horizontal tail it is the average chord length. For the fuselage and tail boom it is their length.

$$c_f = \frac{0.455}{\left(\log_{10} \text{Re}\right)^{2.58}} \tag{22}$$

$$\text{Re} = \frac{\rho V l}{\mu} \tag{23}$$

The form factor for the wing and tail surfaces is based on the maximum thickness (t_{max}) of the airfoil cross-section and its chord length (c). This relation, given by equation 24 for the wing and equation 25 for the tail surfaces, assumes low subsonic Mach number flight ($\sim \leq 0.5$) and a straight wing aircraft configuration. For the fuselage and tail, the form factor is based on their length (l) and diameter (d) and is given by equation 26 [8].

$$F = 1 + 2\frac{t_{max}}{c} + 100\left(\frac{t_{max}}{c}\right)^4 \tag{24}$$

$$F = \left(1 + 2\frac{t_{max}}{c} + 100\left(\frac{t_{max}}{c}\right)^4\right)1.1 \tag{25}$$

$$F = 1 + 60\left(\frac{d}{l}\right)^3 + \frac{l}{d\,400} \tag{26}$$

The wetted surface area for each of the components will depend on their size and shape. Using the above equations with the wind velocity and environmental conditions at a given altitude, the parasitic drag coefficient can be calculated for the aircraft.

The span efficiency (e, Oswald efficiency factor) for a straight wing aircraft is given by equation 27 [9].

$$e = 1.78\left(1 - 0.045\,A_R{}^{0.68}\right) - 0.64 \tag{27}$$

The total efficiency of the propulsion system drive train (η_p) is the combination of the efficiencies of the various pieces within the system. The propulsion system efficiency is given by equation 28. The individual component efficiencies include the motor controller efficiency (η_{mc}), electric motor efficiency (η_{em}), gearbox efficiency (η_g), and propeller efficiency (η_{prop}).

$$\eta_p = \eta_{mc}\eta_{em}\eta_g\eta_{prop} \tag{28}$$

The operational efficiency associated with each of these components is given in table 5. The efficiencies listed consist of the drive-line, which is all of the components up to the propeller. The propeller efficiency has to be calculated based on the propeller sizing and operational altitude. These efficiencies are representative approximations for each of the components under optimized operating conditions. They can be used in the performance assessment of the aircraft over a range of flight conditions. Once a specific design point has been selected, the efficiencies can be adjusted to better reflect that specific operating point.

Table 5.—Drive line component efficiencies.

Component	Efficiency	
Control Electronics	η_{mc}	0.98
Motor	η_{em}	0.90
Gearbox	η_g	0.90
Drive Line Efficiency	η_p	0.794

The last component in the drive train is the propeller. To determine the efficiency of the propeller, it must be sized to meet the thrust requirements of the aircraft. Sizing the propeller is an iterative process that is dependent on the aircraft flight speed and thrust requirement. To achieve the desired thrust at the needed airspeed the propeller diameter, RPM and pitch angle are iterated upon. The goal is to provide a combination of these that maximizes efficiency. To begin the process, an initial propeller design has to be established. This design includes the airfoil selection, and twist and chord length distribution from the root to the tip. The twist and chord length will scale proportionally for changes in propeller diameter. For this analysis, a propeller based on an SD8000-PT airfoil was chosen. Details on this baseline propeller geometry can be found in reference 11. Using this baseline geometry and a vortex theory analysis, the thrust coefficient (c_t) and power coefficients (c_p) were plotted over an advance ratio (J) range from 1.3 to 3 for blade angles of 32° to 48° [12]. These plots were generated for a 2-bladed propeller and are shown in figures 16 and 17. The analysis was limited to a 2-bladed propeller due to aeroshell packaging constraints.

Using figures 16 and 17 and the following relationships for advance ratio, thrust coefficient and power coefficient (given in equations 29 through 31), the propeller diameter and operational revolutions per second (*n*) can be determined. From this the operational efficiency, given by equation 32, can be calculated.

$$J = \frac{V}{nd} \tag{29}$$

$$c_t = \frac{T}{\rho n^2 d^4} \tag{30}$$

$$c_p = \frac{P_r}{\rho n^3 d^5} \tag{31}$$

$$\eta_{prop} = \frac{c_t J}{c_p} \tag{32}$$
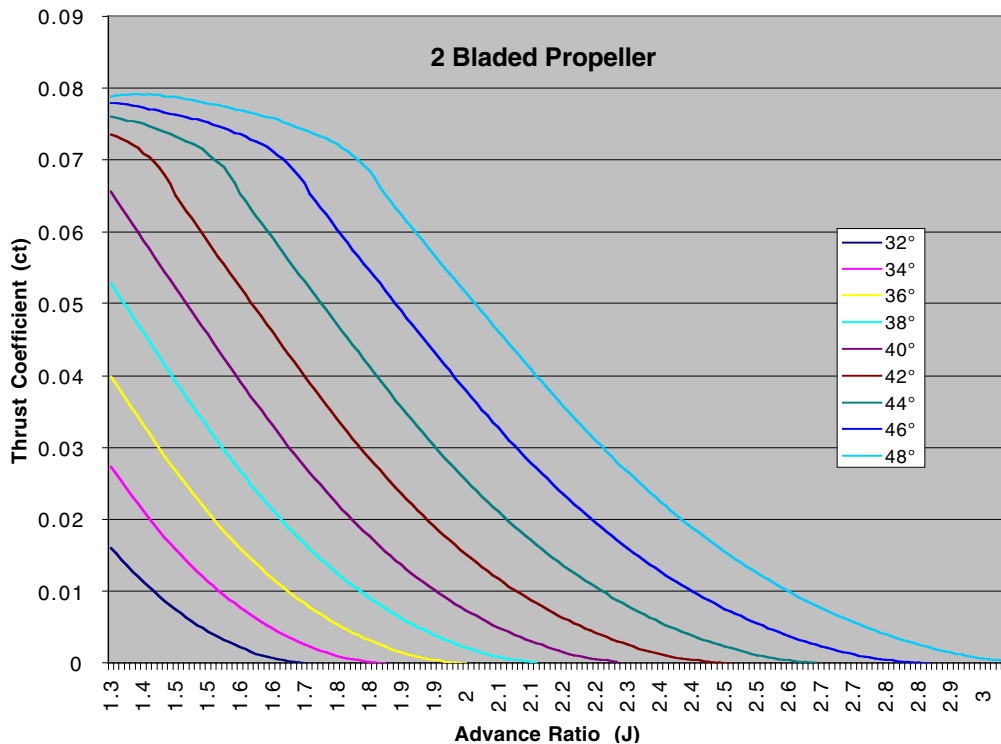
Figure 16.—Propeller thrust coefficient vs. advanced ratio for a 2 bladed propeller.
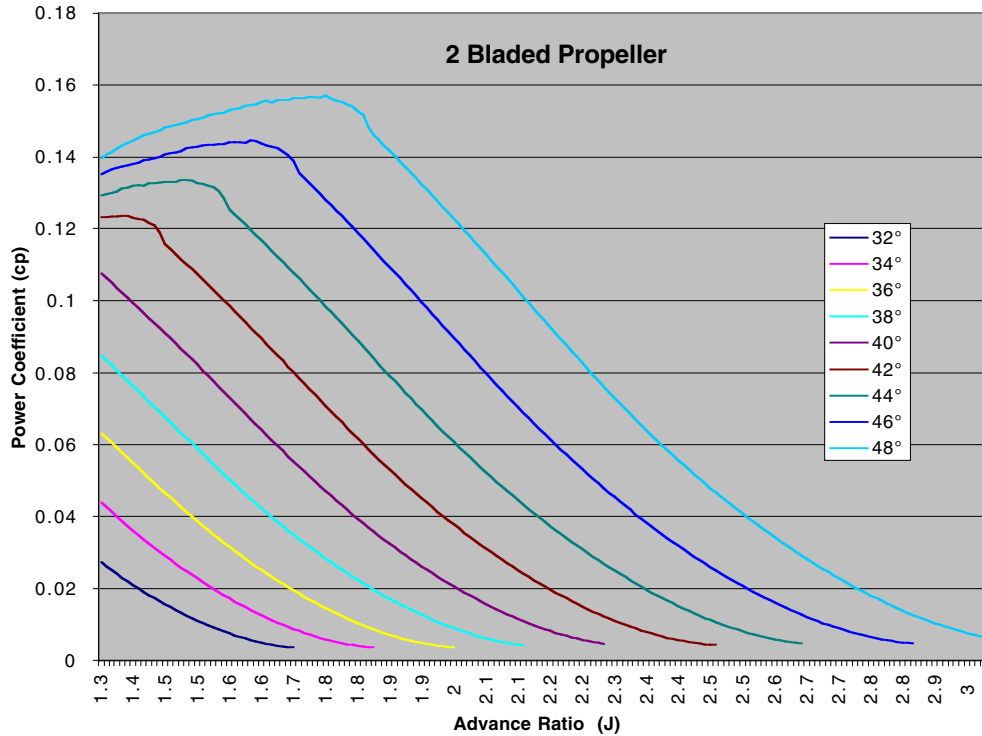
Figure 17.—Propeller power coefficient vs. advance ration for a 2 bladed propeller.

The next step in determining the power required for the aircraft to fly is estimating its total mass. Unlike the airship, the total mass of the aircraft is a critical factor in its feasibility. The mass determines the amount of lift that is needed, which in turn sets the cruise speed of the aircraft and therefore required power. Since the aircraft will be sized for each operating altitude, providing an accurate mass estimate for the aircraft that is easily scalable is necessary for evaluating the aircraft's feasibility under various flight conditions. To estimate the mass, the aircraft was broken down into twelve areas or components plus the payload. Some of these components were assumed to be fixed masses and did not scale with the operating location or aircraft size. These fixed mass components are listed in table 6.

Table 6.—Aircraft fixed component masses.

Component	Mass (kg)
Flight Control Computer	**3.8**
Communications Equiptment	**4.6**
Flight Control Sensors	**3.5**
Payload	**10.0**

Because the masses of some of the components will depend on the aircraft's total mass (M_{ac}) and or power requirement, determining the total mass is an iterative process. The masses of the following items, which include the airframe mass (M_{af}) [10], electric motor mass (M_{em}) [11], motor controller mass (M_{mc}) [11], gearbox mass (M_g) [11], propeller mass (M_{prop}), battery mass (M_b), mass of the power conditioning system (M_{pc}) [6], solar array mass (M_{sa}), and the mass margin, are represented by equations 33 though 40. These items scale with either the aircraft size, power required, and/or total mass.

$$M_{af} = 1.2421 \frac{S_w}{A_R^{0.5}} + 0.4078 M_{ac}^{0.87} \left(\frac{A_R}{S_w}\right)^{0.36} + 0.0026 A_R^{0.9} (1 + 0.008 A_R) M_{ac} +$$

$$0.0998 (A_R S_w)^{0.5} + \left(0.2055 + 0.0028 \left(\frac{A_R}{S_w}\right)^{0.5}\right) S_w + 1.033 S_w^{0.6} \tag{33}$$

$$M_{em} = \frac{P_r \eta_{mc}}{1291} \tag{34}$$

$$M_{mc} = \frac{P_r}{6233} \tag{35}$$

$$M_g = \frac{P_r \eta_{em} \eta_{mc}}{3278} \tag{36}$$

$$M_{pc} = \frac{P_r}{1000} \tag{37}$$

The solar array mass is given by the specific mass of the array in kilograms per meter squared (estimated to be 1 kg/m^2) multiplied by the total solar array area. For this analysis it was assumed that the total array area was 80 percent of the wing and tail area (S_t).

$$M_{sa} = (S_w + S_t) 0.8 \tag{38}$$

The battery sizing is based on a silver-zinc rechargeable battery that has the capacity to provide 5 minutes of full operational power to the aircraft with a depth of discharge of 80 percent. The silver-zinc battery was chosen because of its very high discharge rate capability and its operating temperature range of –20 °C to +30 °C. This type of battery has an estimated energy density of 150 W-Hr/kg. Using this energy density and the 5-minute full power capacity, the mass of the battery can be calculated.

$$M_b = P_r 6.94E - 4 \tag{39}$$

The propeller mass is based on the propeller diameter and the number of blades. The diameter is determined through equations 29 through 31 in the efficiency analysis. With the diameter known the mass of the propeller will depend on the volume of each blade and the material density (ρ_{prop}) it is constructed of. The blade volume can be calculated from the airfoil cross-section that is based on the airfoil chord length (c_{prop}) number of blades (n_b) and the void percentage within the blade (F_b). Using the airfoil cross-sectional area and the chord length distribution given in reference 11, the volume of the propeller blade (V_{prop}) can be calculated. The total propeller mass is given by equation 40. For this analysis it was assumed that a carbon composite, with a density of 1380 kg/m^3, is used to construct the propeller. A 2-bladed propeller is used and the void percentage within the blade is 50 percent.

$$M_{prop} = \rho_{prop} n_b (1 - F_b) \sum_{r=0}^{r=R} \Delta r_i \, 0.0584 c_{prop_i}^2 \tag{40}$$

The last mass item is the margin mass. This is used to account for various miscellaneous items and is assumed to be 10 percent of the calculated aircraft mass. Using this mass margin, total aircraft mass (M_t) is given by equation 41.

$$M_t = \left(21.9 + M_{af} + M_{em} + M_{mc} + M_g + M_{pc} + M_{sa} + M_b + M_{prop}\right)1.1 \qquad (41)$$

Using the analysis method outlined above, three aircraft of different sizes were evaluated to determine their altitude flight range within the Venus atmosphere. Each aircraft had an aspect ratio of 5. The aircraft size was scaled by changing the length of the wingspan. The wingspans used were 6 m, 9 m, and 12 m. The same system power levels used in the airship analysis were used for the aircraft. These are given in table 3. The flight envelope was determined by calculating the power required by the aircraft to fly at a speed equal to the wind speed plus the systems power requirements and comparing that to the power available from the solar array for continuous operation. Figure 18 presents curves, for each aircraft size considered, that show power required and power available over the altitude range from the surface up to 80 km.

From this figure it can be seen that over most of the atmospheric altitude range, from about 10 km to approximately 72 km in altitude, a solar powered aircraft will not have sufficient power to fly faster than the wind speed. Below 10 km in altitude, the curve indicates that there is abundant power for flight. This is due to the very low wind speeds near the surface of the planet, as shown in figure 6. However in this region, the power available curves are very optimistic. Several factors will come into play to significantly reduce the available power from the solar array within this region. Initially the high atmospheric temperatures near the surface will degrade the performance of the solar array. Secondly, the spectrum of the light that makes it through the clouds to the surface is not suited for the operation of conventional solar cells. A special type of solar cell would need to be developed that can take advantage of the light spectrum available near the surface of Venus.
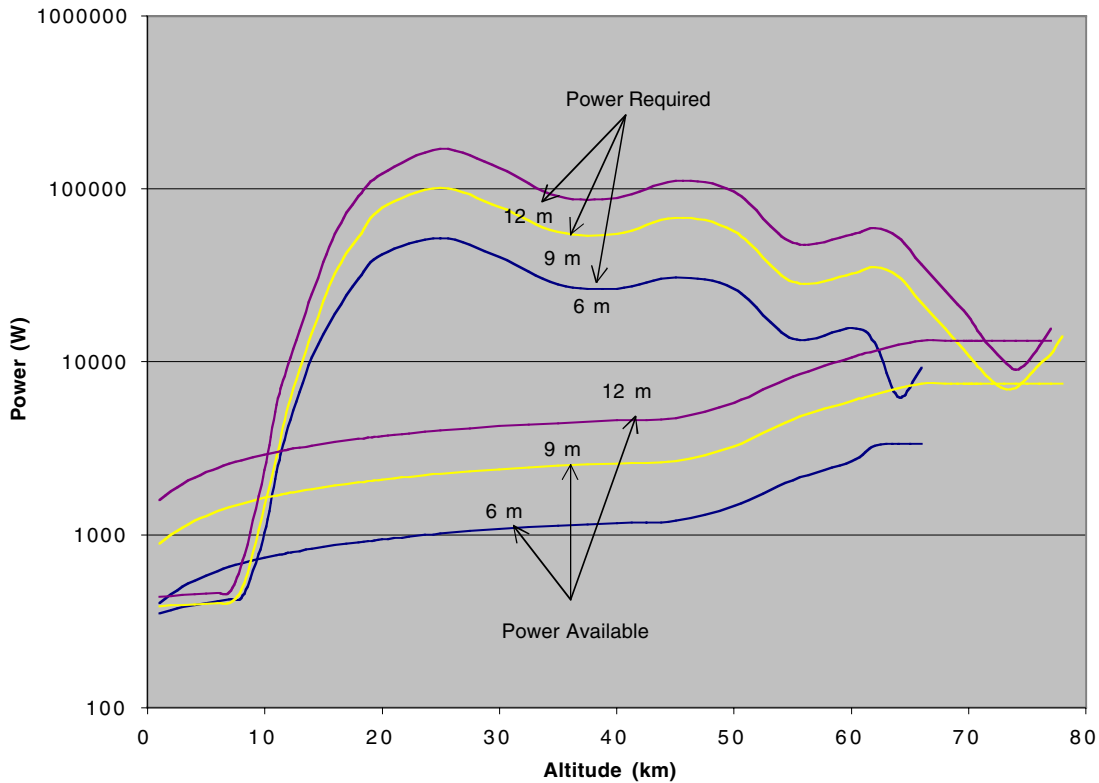
Figure 18.—Solar aircraft power available and power required.
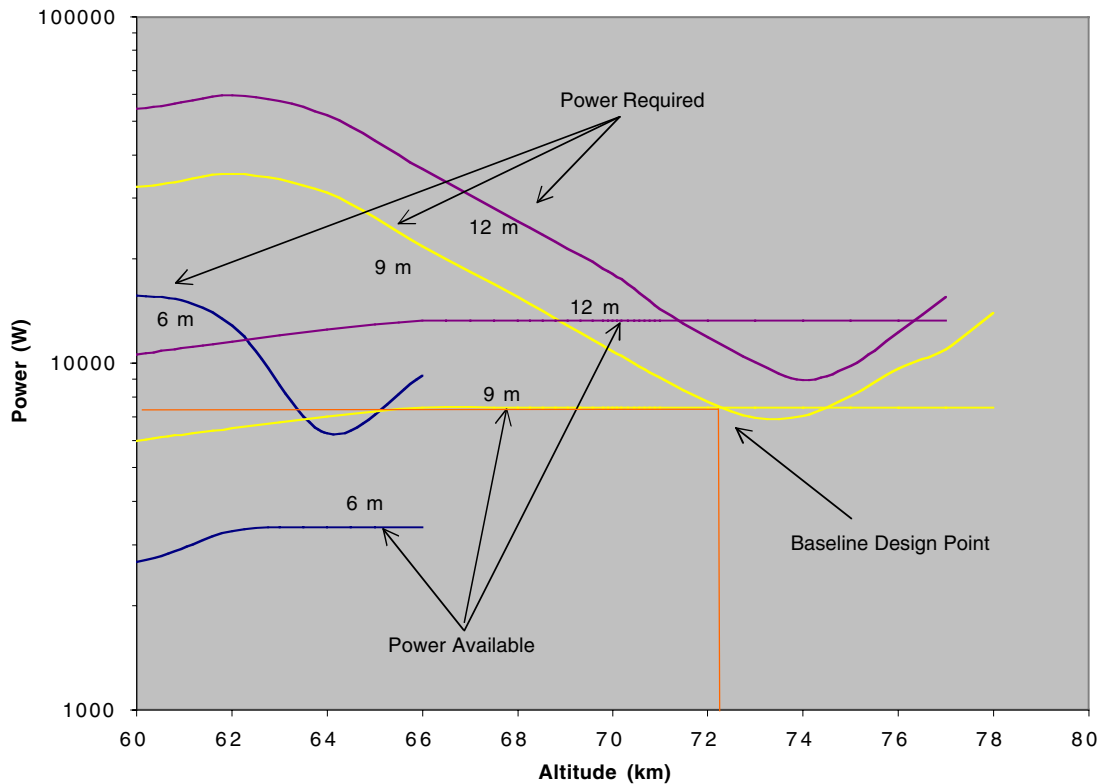
Figure 19.—Venus solar aircraft baseline design point.

There is a second region, upwards of 70 km in altitude, where there is sufficient power to fly faster then the wind speeds. The altitude range where this is feasible depends on the aircraft size. For the aircraft sizes examined, the 9 m and 12 m wingspan aircraft were capable of faster then wind flight within this upper region, whereas the 6 m wingspan aircraft was not.

A close-up of the power required and available curves over this altitude region is shown in figure 19. A baseline design point is indicated on this figure. This design point represents a reference solar powered aircraft configuration that is capable of sustained flight over a single location on Venus. Details on this design point are given in appendix B.

Summary

From the results presented above, the operational ranges and potential feasibility for a solar powered airship and aircraft were determined. The operational ranges were based on a 50-day station-keeping mission. The airship would only be feasible for station-keeping operation at altitudes below 10 km. The aircraft had an operational range from the surface up to 10 km and then from 71 km to 76 km (depending on the aircraft size). Although low altitude operation for both types of vehicles was feasible based on the assumptions used, there are significant issues that would need to be addressed with getting a solar powered air vehicle to operate near the surface of Venus. The main issue is the high atmospheric temperature. Significant materials development would be needed for the vehicle to operate for prolonged periods of time within this high temperature environment. The second and equally critical issue is the operation of solar cells within the environment near the surface. Solar cell performance generally increases with lower operational temperatures. Therefore it may be very difficult to produce any reasonable efficiency out of a solar array operating at such high temperatures. In addition to the temperature, the spectrum of light reaching the surface is mostly on the red side of the spectrum due to the very thick atmosphere. Very little blue light reaches the surface. However it is this blue portion of the

spectrum the most present day solar cells utilize in producing power. To take advantage of the light that does reach the surface, a new type of solar cell would need to be developed.

Aircraft operation within the upper atmosphere would be the best choice for a solar powered air vehicle on Venus. At the altitude range where it can operate and station-keep, it is cold (53 °C) and there is abundant sunlight. The cold temperature operation will enhance the performance of the solar array and the full solar spectrum is available so that conventional solar cells will operate fine. The small operational altitude range would seem like a disadvantage. However it should be understood that this is the range in which the aircraft can fly faster then the wind. This doesn't mean it cannot fly outside this range, just that if it does it will gradually be blown backward by the wind. So the aircraft could conceivably descend to lower altitudes (even into the cloud layer) for brief periods of time then ascend to its operational altitude range where it can regain any ground lost during flight at lower altitudes.

References

1. Windows to the Universe, at http://www.windows.ucar.edu/, University Corporation for Atmospheric Research, July 2002.
2. Ekonomov, A., Golovin, Y., Moroz, V. and Moshkin, B., "19: Solar Scattered Radiation Measurements by Venus Probes," Journal Venus, University of Arizona Press 1983.
3. Landis, G.A., Colozza A., LaMarre, M.C., "Atmospheric Flight on Venus," NASA/TM—2002-211467, June 2002.
4. "Space and Planetary Environment Criteria Guidelines for Use in Space Vehicle Development 1982 Revision (Volume 1)," NASA TM–82478, January 1983.
5. Personal Correspondence with Viktor. V. Kerzhanovich, JPL, January 2000.
6. Colozza, A.J., "Initial Feasibility Assessment of a High Altitude Long Endurance Airship," NASA contractor report, under publication, October 2003.
7. McCormick, B.W., Aerodynamics, Aeronautics and Flight Mechanics John Wiley & Sons Publisher, 1979.
8. Raymer, D.P., Aircraft Design: A Conceptual Approach, AIAA Education Series, 1989.
9. Cavallok, B., "Subsonic Drag Estimation Methods," US Naval Air Development Center, NADC-AW-6604, 1966.
10. Colozza, A.J., "Effect of Power System Technology and Mission Requirements on High Altitude Long Endurance Aircraft," NASA CR-194455, February 1994.
11. Colozza, A.J., "Comparison of Mars Aircraft Propulsion Systems," NASA/CR—2003-212350, May 2003.
12. Colozza, A.J., "High Altitude Propeller Design and Analysis Overview," NASA/CR—1998-208520, October 1998.

Appendix A
Mean Standard Atmosphere for Venus (JPL Model) [4]

H Km	T K	P (bar)	r kg/m³	U m/s	m Pa*s	n s/m²	Cp J/kg*K	Cp/Cv	A m/s	K W/m*K
0	735.3	92.1	64.79	0.6	3.35E-05	5.17E-07	1181	1.193	410	0.0588
1	727.7	86.45	61.56	0.7	3.12E-05	5.07E-07	1177	1.194	408	0.0575
2	720.2	81.09	58.45	0.8	2.89E-05	4.95E-07	1172	1.195	406	0.0561
3	712.4	76.01	55.47	0.9	2.67E-05	4.81E-07	1168	1.196	404	0.0548
4	704.6	71.2	52.62	1.0	2.44E-05	4.63E-07	1163	1.197	402	0.0534
5	696.8	66.65	49.87	1.2	2.21E-05	4.43E-07	1159	1.198	400	0.0521
6	688.8	62.35	47.24	1.3	2.18E-05	4.62E-07	1155	1.199	398	0.0511
7	681.1	58.28	44.71	1.9	2.16E-05	4.83E-07	1151	1.200	396	0.0501
8	673.6	54.44	42.26	2.4	2.13E-05	5.04E-07	1146	1.200	393	0.0490
9	665.8	50.81	39.95	3.4	2.11E-05	5.27E-07	1142	1.201	391	0.0480
10	658.2	47.39	37.72	4.5	2.08E-05	5.51E-07	1138	1.202	389	0.0470
11	650.6	44.16	35.58	6.3	2.25E-05	6.33E-07	1134	1.203	387	0.0462
12	643.2	41.12	33.54	8.2	2.42E-05	7.23E-07	1129	1.204	385	0.0455
13	635.5	38.26	31.6	10.8	2.60E-05	8.22E-07	1125	1.205	383	0.0447
14	628.1	35.57	29.74	13.4	2.77E-05	9.31E-07	1120	1.206	381	0.0440
15	620.8	33.04	27.95	16.1	2.94E-05	1.05E-06	1116	1.207	379	0.0432
16	613.3	30.66	26.27	19.6	2.91E-05	1.11E-06	1111	1.208	377	0.0425
17	605.2	28.43	24.68	22.0	2.88E-05	1.17E-06	1106	1.209	374	0.0417
18	597.1	26.33	23.18	24.5	2.84E-05	1.23E-06	1101	1.211	372	0.0410
19	589.3	24.36	21.74	26.0	2.81E-05	1.29E-06	1096	1.212	369	0.0402
20	580.7	22.52	20.39	27.6	2.78E-05	1.36E-06	1091	1.213	367	0.0395
21	572.4	20.79	19.11	28.8	2.76E-05	1.44E-06	1085	1.214	365	0.0388
22	564.3	19.17	17.88	29.9	2.74E-05	1.53E-06	1079	1.216	362	0.0382
23	556.0	17.66	16.71	30.6	2.71E-05	1.62E-06	1074	1.217	360	0.0375
24	547.5	16.25	15.62	31.3	2.69E-05	1.72E-06	1068	1.219	357	0.0369
25	539.2	14.93	14.57	32.3	2.67E-05	1.83E-06	1062	1.220	355	0.0362
26	530.7	13.7	13.59	33.3	2.64E-05	1.94E-06	1056	1.222	352	0.0357
27	522.3	12.56	12.65	34.0	2.61E-05	2.06E-06	1049	1.223	350	0.0352
28	513.8	11.49	11.77	34.6	2.58E-05	2.19E-06	1043	1.225	347	0.0346
29	505.6	10.5	10.93	35.0	2.55E-05	2.33E-06	1036	1.226	345	0.0341
30	496.9	9.851	10.15	35.5	2.52E-05	2.48E-06	1030	1.228	342	0.0336
31	488.3	8.729	9.406	36.0	2.49E-05	2.65E-06	1023	1.230	339	0.0331
32	479.9	7.94	8.704	36.4	2.46E-05	2.83E-06	1016	1.232	337	0.0325
33	472.7	7.211	8.041	36.7	2.44E-05	3.03E-06	1010	1.234	334	0.0320
34	463.4	6.537	7.42	36.9	2.41E-05	3.25E-06	1003	1.236	332	0.0314
35	455.5	5.917	6.831	37.3	2.38E-05	3.48E-06	996	1.238	329	0.0309
36	448.0	5.346	6.274	37.6	2.35E-05	3.75E-06	990	1.240	326	0.0304
37	439.9	4.822	5.762	38.2	2.33E-05	4.04E-06	983	1.242	324	0.0300

H Km	T K	P (bar)	r kg/m³	U m/s	m Pa*s	n s/m²	Cp J/kg*K	Cp/Cv	A m/s	K W/m*K
38	432.5	4.342	5.276	38.7	2.30E-05	4.36E-06	977	1.244	321	0.0295
39	425.1	3.903	4.823	39.7	2.28E-05	4.72E-06	970	1.246	319	0.0291
40	417.6	3.501	4.404	40.7	2.25E-05	5.11E-06	964	1.248	316	0.0286
41	410.0	3.135	4.015	42.6	2.23E-05	5.55E-06	958	1.250	314	0.0282
42	403.5	2.802	3.646	44.5	2.21E-05	6.05E-06	953	1.252	311	0.0277
43	397.1	2.499	3.303	47.4	2.18E-05	6.61E-06	947	1.253	309	0.0273
44	391.2	2.226	2.985	50.3	2.16E-05	7.24E-06	942	1.255	306	0.0268
45	385.4	1.979	2.693	54.2	2.14E-05	7.95E-06	936	1.257	304	0.0264
46	379.7	1.756	2.426	57.4	2.11E-05	8.71E-06	930	1.259	302	0.0260
47	373.1	1.556	2.186	59.4	2.09E-05	9.55E-06	923	1.261	299	0.0256
48	366.4	1.375	1.967	61.0	2.06E-05	1.05E-05	917	1.264	297	0.0251
49	358.6	1.213	1.769	61.2	2.04E-05	1.15E-05	910	1.266	294	0.0247
50	350.5	1.066	1.594	60.9	2.01E-05	1.26E-05	904	1.268	292	0.0243
51	342.0	0.9347	1.432	60.2	1.97E-05	1.38E-05	895	1.272	288	0.0239
52	333.3	0.8167	1.284	59.4	1.94E-05	1.51E-05	886	1.276	284	0.0235
53	323.0	0.7109	1.153	59.3	1.90E-05	1.65E-05	877	1.279	281	0.0231
54	312.8	0.616	1.032	59.2	1.87E-05	1.81E-05	868	1.283	277	0.0227
55	302.3	0.5314	0.9207	59.9	1.83E-05	1.99E-05	859	1.287	273	0.0223
56	291.8	0.4559	0.8183	60.5	1.80E-05	2.20E-05	851	1.290	270	0.0219
57	282.5	0.3891	0.7212	62.7	1.77E-05	2.45E-05	844	1.294	266	0.0215
58	275.2	0.3306	0.6289	65.0	1.73E-05	2.76E-05	836	1.297	263	0.0212
59	268.7	0.2796	0.5448	71.1	1.70E-05	3.12E-05	829	1.301	259	0.0208
60	262.8	0.2357	0.4694	77.2	1.67E-05	3.56E-05	821	1.304	256	0.0204
61	258.7	0.2008	0.40525	85.4	1.66E-05	4.09E-05	818	1.306	255	0.0201
62	254.5	0.1659	0.3411	92.0	1.64E-05	4.82E-05	815	1.307	253	0.0197
63	250.0	0.14075	0.2927	94.0	1.63E-05	5.57E-05	811	1.309	252	0.0194
64	245.4	0.1156	0.2443	94.5	1.62E-05	6.62E-05	808	1.310	250	0.0190
65	243.2	0.09765	0.2086	95.0	1.61E-05	7.69E-05	805	1.312	249	0.0187
66	241.0	0.0797	0.1729	94.4	1.59E-05	9.21E-05	802	1.314	247	0.0184
67	238.2	0.06709	0.14695	93.8	1.58E-05	1.07E-04	799	1.315	246	0.0180
68	235.4	0.05447	0.121	93.2	1.57E-05	1.29E-04	795	1.317	244	0.0177
69	232.6	0.04569	0.102465	92.6	1.55E-05	1.52E-04	792	1.318	243	0.0173
70	229.8	0.0369	0.08393	92.0	1.54E-05	1.83E-04	789	1.320	241	0.0170
71	227.0	0.03083	0.07084	89.4	1.53E-05	2.15E-04	786	1.322	239	0.0167
72	224.1	0.02476	0.05775	86.8	1.51E-05	2.61E-04	783	1.324	238	0.0164
73	221.4	0.02061	0.04854	84.2	1.50E-05	3.08E-04	779	1.325	236	0.0161
74	218.6	0.01645	0.03933	81.6	1.48E-05	3.76E-04	776	1.327	235	0.0158
75	215.4	0.01363	0.03298	79.0	1.47E-05	4.44E-04	773	1.329	233	0.0155
76	212.1	0.01081	0.02663	74.6	1.45E-05	5.44E-04	770	1.331	231	0.0151
77	208.7	0.00891	0.022235	70.2	1.44E-05	6.45E-04	767	1.333	230	0.0148

H Km	T K	P (bar)	r kg/m³	U m/s	m Pa*s	n s/m²	Cp J/kg*K	Cp/Cv	A m/s	K W/m*K
78	205.3	0.00701	0.01784	65.8	1.42E-05	7.96E-04	763	1.334	228	0.0145
79	201.2	0.00589	0.01485	61.4	1.41E-05	9.46E-04	760	1.336	227	0.0142
80	197.1	0.00476	0.01186	57.0	1.39E-05	1.17E-03	757	1.338	225	0.0139
81	193.5	0.00378	0.009793	52.4	1.38E-05	1.41E-03	755	1.340	223	0.0138
82	189.9	0.00281	0.007725	47.8	1.36E-05	1.77E-03	752	1.341	222	0.0136
83	186.9	0.00227	0.006326	43.2	1.35E-05	2.14E-03	750	1.343	220	0.0135
84	183.8	0.00173	0.004926	38.6	1.34E-05	2.72E-03	747	1.344	219	0.0133
85	181.0	0.00139	0.004007	34.0	1.33E-05	3.31E-03	745	1.346	217	0.0132
86	178.2	0.00105	0.003088	30.4	1.31E-05	4.25E-03	743	1.347	215	0.0131
87	175.9	0.00084	0.002493	26.8	1.30E-05	5.21E-03	740	1.349	214	0.0129
88	173.6	0.00063	0.001898	23.2	1.29E-05	6.78E-03	738	1.350	212	0.0128
89	171.5	0.0005	0.001525	19.6	1.27E-05	8.35E-03	735	1.352	211	0.0126
90	169.4	0.00037	0.001151	16.0	1.26E-05	1.09E-02	733	1.353	209	0.0125
91	168.3	0.0003	0.000917	15.0	1.26E-05	1.38E-02	734	1.353	209	0.0125
92	167.2	0.00022	0.000684	14.0	1.27E-05	1.85E-02	734	1.353	210	0.0126
93	167.2	0.00017	0.000542	13.0	1.27E-05	2.34E-02	735	1.353	210	0.0126
94	167.2	0.00013	0.0004	12.0	1.27E-05	3.18E-02	735	1.353	211	0.0126
95	168.2	0.0001	0.000315	11.0	1.28E-05	4.04E-02	736	1.353	211	0.0127
96	169.2	7.5E-05	0.000231	10.8	1.28E-05	5.52E-02	736	1.352	211	0.0127
97	170.6	6E-05	0.000183	10.6	1.28E-05	7.00E-02	737	1.352	212	0.0127
98	172.0	4.5E-05	0.000135	10.4	1.28E-05	9.53E-02	737	1.352	212	0.0127
99	173.7	3.6E-05	0.000107	10.2	1.29E-05	1.21E-01	738	1.352	213	0.0128
100	175.4	2.7E-05	7.89E-05	10.0	1.29E-05	1.63E-01	738	1.352	213	0.0128

Appendix B
Solar Powered Aircraft Baseline Design Point Sizing Output

Power

Max Powr Available	7460.2181
Total Power Required	7400.654
Propulsion Power Required at Wind speed	7250.654
Excess Payload Power Available	59.564084
Payload Power	50
Communications Power	50
Aircraft Systems Power	50
Power To Propeller	5755.5691
Control Electronics Efficiency	0.98
Motor Efficiency	0.9
Gearbox Efficiency	0.9
Propeller Efficiency	0.8375944
Propeller & Engine Eff.	0.6648824

Propeller

Propeller Diameter	2.9417135
Number of Blades	2
Maximum Tip Mach Number	0.8
Advance Ratio	1.624734

Mass Breakdown

Airframe mass	35.423594
Flight Control Computer Mass	3.8
Electric Motor Mass	5.5039821
Motor Controller Mass	1.1632687
Gearbox Mass	1.9509081
Propeller Mass	3.2521355
Battery Mass	5.0351764
Communications equipment Mass	4.6
Power Conditioning Mass	7.250654
Solar Array Mass	15.857793
Flight Contol Sensors Mass	3.5
Mass Margin	8.7337511
Payload Mass	10
Total Mass	106.07126

Environment

Speed Of Sound	235.66129
Altitude	72
Wind Velocity	86.604981
Density (kg/m^3)	0.0631861
Attentunation Factor	1

Solar Array

Solar Cell Eff	0.18
PV Cell Row Spacing (m)	0.06667
Fill Factor wing	0.8
Fill Factor Tail	0.8
Solar Cell Area (m^2)	15.857793

Performance

V steady level flight (m/s)	69.855539
V min Thrust or Max L/D	69.450331
Vstall (m/s)	34.99329
Liftoff Speed (m/s)	38.49262
V(m/s) for Min Power	52.77084
V vert (sink rate) m/s	4.1221107
Lift/Drag (cruise)	16.902193
Lift/Drag (max)	18.576362

Sizing

Wing Area (m^2)	16.213235
Weight (N)	940.85392
W/S (N/m^2)	58.029993
Aspect Ratio Wing	5
Aspect Ratio Tail	1.5085719
wing span (m)	9.0036757
wing cord (m)	1.8007351
Tail Cord (m)	1.5467167
Horizontal Tail Length (m)	2.3333333
Vertical Tail Heigh (m)	0.4506759
Tail Moment Arm (m)	4.0448458
Aeroshell Diameter	3.5
Aeroshell Cone Angle	45
Full Battery Operation	5
Mass Margin	0.1

REPORT DOCUMENTATION PAGE

1. AGENCY USE ONLY (*Leave blank*)	2. REPORT DATE	3. REPORT TYPE AND DATES COVERED
	April 2004	Final Contractor Report

4. TITLE AND SUBTITLE

Solar Powered Flight on Venus

6. AUTHOR(S)

Anthony Colozza

5. FUNDING NUMBERS

WBS–22–755–81–01
NAS3–00145

7. PERFORMING ORGANIZATION NAME(S) AND ADDRESS(ES)

Analex Corporation
3001 Aerospace Parkway
Brook Park, Ohio 44142

8. PERFORMING ORGANIZATION REPORT NUMBER

E–14488

9. SPONSORING/MONITORING AGENCY NAME(S) AND ADDRESS(ES)

National Aeronautics and Space Administration
Washington, DC 20546–0001

10. SPONSORING/MONITORING AGENCY REPORT NUMBER

NASA CR—2004–213052

11. SUPPLEMENTARY NOTES

Project Manager, Geoff Landis, Power and On-Board Propulsion Technology Division, NASA Glenn Research Center, organization code 5410, 216–433–2238.

12a. DISTRIBUTION/AVAILABILITY STATEMENT

Unclassified - Unlimited
Subject Categories: 07, 44, and 05   Distribution: Nonstandard

Available electronically at http://gltrs.grc.nasa.gov

This publication is available from the NASA Center for AeroSpace Information, 301–621–0390.

12b. DISTRIBUTION CODE

13. ABSTRACT (*Maximum 200 words*)

Solar powered flight within the Venus environment from the surface to the upper atmosphere was evaluated. The objective was to see if a station-keeping mission was possible within this environment based on a solar power generating system. Due to the slow rotation rate of Venus it would be possible to remain within the day light side of the planet for extended periods of time. However the high wind speeds and thick cloud cover make a station-keeping solar powered mission challenging. The environment of Venus was modeled as a function of altitude from the surface. This modeling included density, temperature, solar attenuation and wind speed. Using this environmental model flight with both airships and aircraft was considered to evaluate whether a station-keeping mission is feasible. The solar power system and flight characteristics of both types of vehicles was modeled and power balance was set up to determine if the power available from the solar array was sufficient to provide enough thrust to maintain station over a fixed ground location.

14. SUBJECT TERMS

Venus atmosphere; Solar powered aircraft

15. NUMBER OF PAGES

33

16. PRICE CODE

17. SECURITY CLASSIFICATION OF REPORT	18. SECURITY CLASSIFICATION OF THIS PAGE	19. SECURITY CLASSIFICATION OF ABSTRACT	20. LIMITATION OF ABSTRACT
Unclassified	Unclassified	Unclassified	